



Published in final edited form as:

*Circ Cardiovasc Imaging*. 2008 September ; 1(2): 94–103. doi:10.1161/CIRCIMAGING.108.797449.

## Serial Noninvasive In Vivo Positron Emission Tomographic Tracking of Percutaneously Intramyocardially Injected Autologous Porcine Mesenchymal Stem Cells Modified for Transgene Reporter Gene Expression

Mariann Gyöngyösi, MD, PhD, FESC, Jeronimo Blanco, PhD, Teréz Marian, MD, Lajos Trón, MD, Örs Petneházy, PhD, Zsolt Petrasi, PhD, Rayyan Hemetsberger, MD, Julio Rodriguez, PhD, Gusztáv Font, VMD, Imre J. Pavo, István Kertész, MD, László Balkay, MD, Noemi Pavo, MSc, Aniko Posa, PhD, Miklos Emri, PhD, László Galuska, PhD, Dara L. Kraitchman, VMD, PhD, Johann Wojta, PhD, Kurt Huber, MD, FESC, FACC, and Dietmar Glogar, MD, FESC

From the Department of Cardiology, Medical University of Vienna, Austria (M.G., R.H., I.J.P., N.P., A.P., J.W., D.G.); Centro de Investigación Cardiovascular (CSIC-ICCC), CIBER-BBN, Barcelona, Spain (J.B., J.R.); PET Centrum—Institute of Nuclear Medicine of the University of Debrecen, Hungary (T.M., L.T., I.K., L.B., M.E., L.G.); Institute of Diagnostic Imaging and Radiation Oncology, University of Kaposvar, Hungary (O.P., Z.P.); Downtown Animal Clinic, Budapest, Hungary (G.F.); The Johns Hopkins University, School of Medicine, Russell H. Morgan Department of Radiology and Radiological Science, Baltimore, MD (D.L.K.); 3rd Department of Medicine (Cardiology and Emergency Medicine), Wilhelminenhospital, Vienna, Austria (K.H.)

### Abstract

**Background**—Porcine bone marrow-derived mesenchymal stem cells (MSCs) were stably transfected with a lentiviral vector for transgene expression of the trifusion protein renilla luciferase, red fluorescent protein and herpes simplex truncated thymidine kinase (LV-RL-RFP-tTK; positron emission tomography [PET] reporter gene) for in vivo noninvasive tracking of the intramyocardially delivered MSC fate.

**Methods and Results**—A closed-chest, reperfused myocardial infarction was created in farm pigs. Sixteen days after myocardial infarction, LV-RL-RFP-tTK-MSCs were injected intramyocardially using electromechanical mapping guidance in the infarct border zone (n=7). PET-computed tomographic metabolic and perfusion imaging was performed after an intravenous injection of 10 mCi [18F]-FHBG and 13N-ammonia PET at 30±2 hours and 7 days after LV-RL-RFP-tTK-MSC treatment. Fusion imaging of the [18F]-FHBG PET-computed tomography with MRI was used to determine the myocardial location of the injected LV-RL-RFP-tTK-MSCs. Seven days after injections, [18F]-FHBG PET showed a decreased cardiac uptake with a mild increased pericardial and pleura uptake in the treated animals, which was confirmed by the measurement of luciferase activity. At 10 days, infarct size by MRI in the LV-RL-RFP-tTK-MSC-treated animals was smaller than controls (n=7) (23.3±1.5% versus 30.2±3.5%,  $P<0.005$ ). The presence of the LV-RL-RFP-tTK-MSCs (5.8±1.1% of the injected cells) in the myocardium 10 days after intramyocardial delivery was confirmed histologically.

© 2008 American Heart Association, Inc.

Correspondence to Mariann Gyöngyösi, MD, PhD, FESC, Department of Cardiology, Medical University of Vienna, Wahinger Gurtel 18–20, A-1090 Vienna, Austria, mariann.gyongyosi@meduniwien.ac.at.

Reprints: Information about reprints can be found online at <http://www.lww.com/reprints>

**Conclusions**—Reporter gene imaging enables the tracking of the persistence of viable LV-RL-RFP-tTK-MS-C in the peri-infarcted porcine myocardium at 10 days after delivery using clinical PET scanners.

### Keywords

cells; imaging; infarction; mapping; revascularization

Cardiac transplantation of stem cells (SCs) has been shown to improve regional perfusion and systolic function of the failing heart after myocardial infarction (MI).<sup>1,2</sup> However, once delivered to the heart, unlabeled cells cannot be visualized or tracked in vivo. Although iron oxide-labeled SCs can be detected by MRI, this method is insensitive to a small number of cells, is hindered by the label dilution because of cell division and migration, and cannot distinguish live from dead cells.<sup>3-5</sup>

The reporter gene approach is another method to track SC fate noninvasively.<sup>6</sup> Because the reporters are expressed only in living cells and are passed to daughter cells on cell division without dilution, the sensitivity for in vivo detection is enhanced.<sup>6,7</sup> Using a reporter system, multimodality (including bioluminescence, fluorescence, and positron emission tomography [PET]) imaging permits longitudinal monitoring of the cell survival, homing, and quantification over an extended period, if the reporter gene is stably expressed.

Coupling of the reporter gene to tissue specific gene promoters could also allow monitoring of cell differentiation, eg, detection of angiogenic gene expression would be possible.<sup>6</sup>

Because PET reporter gene imaging in a large animal model of MI on a clinical PET scanner has not been demonstrated, the aim of the present study was to adapt and validate the reporter gene method for in vivo monitoring of cardiac SC therapy in a large animal MI model that would facilitate translational research.

## Methods

### Cell Culture

Porcine bone marrow (BM)-derived mesenchymal stem cells (MSCs) were selected from 100 mL BM mononuclear cell fraction using a Ficoll-Paque gradient (Ficoll-Paque, Amersham Biosciences, Uppsala, Sweden) and stored at 4°C in Baxter bag (Baxter Healthcare, Ltd, Thetford, Norfolk, UK) in seven pigs (MSC group). Buffy coats were plated at 50 000 cells/cm<sup>2</sup> in alpha modified Eagle's medium without nucleotides but also containing 10% FCS and 2 mmol/L L-glutamine, penicillin or streptomycin supplemented with 1 ng/mL Fibroblast Growth Factor 2. Cells were harvested by trypsinization when 75% confluent and replated at a cell density of 1000 cells/cm<sup>2</sup>. Cells were tested for absence of CD45 expression. In vitro cell differentiation testing was performed in CD45<sup>-</sup> cultures.

### Differentiation and Characterization of the MSCs Stemness

The differentiation media for adipogenesis consisted of DMEM (low glucose), 20% FCS, 0.5 mmol/L isobutylmethylxanthine, 60 µmol/L indomethacin, and 10 to 6 mol/L dexamethasone. For osteoblastic differentiation, the medium consisted of DMEM (high glucose), 10% FCS, 10 mmol/L β-glycerophosphate, 50 µg/mL L-ascorbic acid, and 10 to 7 mol/L dexamethasone. For chondrogenic differentiation, a micropellet system was used. Cells were suspended in DMEM, containing 0.1 µmol/L dexamethasone, 1 mmol/L sodium pyruvate, 0.17 mmol/L ascorbic acid, 0.35 mmol/L proline, and 1:500 stock from Cambrex of insulin-transferrin-selenium. The medium was supplemented with bone morphogenic protein-2 at 100 ng/mL or transforming growth factor-β at 10 ng/mL (Figure 1).

## Cell Transfection

MSCs were transfected by incubation with cell culture supernatants from 293 T lentiviral packaging cells, previously transfected, using the calcium phosphate method, with the envelope plasmid pMD-G-VSVG, the packaging plasmid pCMV-DR8.2, and an expression plasmid construct containing the renilla luciferase (RL)-red fluorescence protein (RFP)-herpes simplex truncated thymidine kinase (tTK) (LV-RL-RFP-tTK). Fluorescence-activated cell sorting was used to select the highest RFP<sup>+</sup> cells (10% of the total transfected MSC) for in vivo delivery (Figure 1).

## Effect of Reporter Genes on LV-RL-RFP-tTK-MSCs Cell Viability and Proliferation

For cell viability and proliferation assay, the cells were serially washed with PBS (Invitrogen, Carlsbad, Calif), collected at different time points (1 to 30 days and 1 day before cardiac implantation), and viable cells were counted with the trypan blue exclusion assay with a Bürker–Türk hemocytometer. Cell doubling time (Td) was calculated during the log phase of growth curves. The MSCs from each well were counted five times at separated time points, and the results were averaged (Figure 1).

## Preparation of the [18F]-FHBG Tracer

[18F]-labeled 9-[4-fluoro-3-(hydroxymethyl)butyl]guaninderivatives ([18F]-FHBG) was synthesized based on a modified method with a RP-high-performance liquid chromatography final purification and an online sterile filtration.<sup>8</sup> All preparations showed at least 98% radiochemical purity of [18F]-FHBG. The radiochemical yield was 10% to 12% (corrected for decay) in five runs, and the synthesis time was 120 minutes from the end of bombardment. The average specific radioactivity of the radiotracer was 44.4 to 74 GBq/ $\mu$ mol (1.2 to 2 Ci/ $\mu$ M).

For in vitro analysis of the [18F]-FHBG tracer uptake, the LV-RL-RFP-tTK-MSCs, the cells ( $0.5 \times 10^6$ /mL) were incubated at 36°C in PBS containing 5 mmol/L D-glucose and 15  $\mu$ Ci/mL [18F]-FHBG for 20 to 180 minutes. The unbound tracer was washed. The cells were resuspended in 1 mL PBS and loaded in 1-cm diameter tubes after which the activity was counted in a gamma counter (Canberra Packard, Dreieich, Germany) for 1 minute within the 18F-sensitive energy window to determine isotope incorporation.

## Animal Protocol

Fourteen domestic pigs (25 to 30 kg) underwent induction of MI (closed-chest, reperfused model, seven of them had previous BM-harvesting) (Figure 2). The pigs were sedated with 12 mg/kg ketamine hydrochloride, 1 mg/kg xylazine, and 0.04 mg/kg atropine intramuscularly after overnight fasting. Following endotracheal intubation, a 6F introduction sheath (Terumo Medical Corporation, Somerset, NJ) was inserted in the femoral artery. After the administration of 200 IU/kg of heparin, selective angiography of the left coronary arteries was performed, and a balloon catheter (3.0 mm in diameter, 15 mm long) (Maverick, Boston Natick, Mass) was advanced into the left anterior descending coronary artery after the origin of the first major diagonal branch. The mid left anterior descending coronary artery was then occluded by inflation of the balloon at 5 atm for 60 minutes, followed by reperfusion via balloon deflation. After hemodynamic stabilization, the pig was allowed to recover.

Sixteen days after acute MI, after baseline cardiac MRI, seven pigs received 3D NOGA-guided intramyocardial injections of LV-RL-RFP-tTK-MSC (Group LV-RL-RFP-tTK-MSC), whereas seven pigs served as controls (Group Control). For in vivo tracking of the injected cells, [18F]-FHBG PET-computer tomography (CT) imaging was performed 30 $\pm$ 2 hours and 7 days after injections.

Ten days after delivery of the LV-RL-RFP-tTK-MSC, the pigs underwent another MRI and then were humanely euthanized and the hearts excised. The endocardial injection sites were localized and sectioned. Tissue samples of the heart (ie, injection sites, infarcted-noninjected sites, and normal myocardium) and different organs (ie, pericardium, pleura, lung, mediastinal lymphatic nodes, liver, spleen, bone marrow) were collected from all pigs and subjected to either histopathologic cell counting or luciferase assay (Figure 2).

### **Intramyocardial Delivery of Transfected Cells Using 3D NOGA Guidance**

After placement of 8F sheath (Terumo Medical Corporation), the diagnostic electromechanical NOGA mapping catheter (Cordis, a Johnson & Johnson, Miami Lakes, Fla) was introduced into the LV cavity. Detailed descriptions of the endocardial mapping system components are previously published.<sup>9–11</sup>

After the diagnostic NOGA endocardial mapping, the LV-RL-RFP-tTK-MSCs were injected into the peri-infarct myocardium in  $11.3 \pm 1.2$  sites with  $6.3 \pm 1.1 \times 10^5$  cells/injections using the Myostar injection catheter (Cordis, Johnson & Johnson). The injections (0.3 mL cell suspension each) were given slowly (30 to 40 seconds) and only to areas with a unipolar voltage above 5 mV, using the quality control criteria.<sup>9</sup>

### **Cardiac PET Imaging**

For determination of the myocardial perfusion and to facilitate the localization of the injected LV-RL-RFP-tTK-MSC, <sup>13</sup>N-ammonia PET was performed 1 hour before [<sup>18</sup>F]-FHBG PET. After the transmission CT scan, dynamic image acquisition was started simultaneously with the intravenous injection of 500 MBq <sup>13</sup>N-ammonia (12 frames with 10 seconds, three frames with 60 seconds, three frames with 300 seconds). After physical decay of <sup>13</sup>N-ammonia to nearly undetectable activity levels, 10 mCi ( $\approx 0.33$  mCi/kg) [<sup>18</sup>F]-FHBG were injected intravenously, and PET scans were completed 1 hour after tracer injection.

Emission images were summed and analyzed with the transmission PET data by using an ECAT EXACT 921 (CTI/Siemens) scanner over 60 minutes in three-dimensional acquisition mode. For attenuation correction, 15 minutes transmission scans were acquired after completing the dynamic scan. Random-, scatter-, and attenuation-corrected transaxial images were reconstructed by the ordered subset EM (OSEM) method (four iteration, eight subset) supplied by the manufacturer. The uptake of radioactivity was decay corrected and expressed as standard uptake value, normalizing the accumulation to the injected activity and the body weight. Standard uptake value was calculated as activity per milliliter/injected activity/ body weight. Emission images between 40 to 60 minutes were summed and analyzed together with the transmission data by using MATLAB 7.1.

Regional myocardial concentrations (percentage dose per milliliter) were estimated from maximum pixels within the regions of interest (ROIs).<sup>12</sup> The count ratio of [<sup>18</sup>F]-FHBG PET relative to remote myocardium was calculated.<sup>12</sup>

### **Cardiac MRI of the Pigs**

Cardiac MRI was performed using a 1.5-T clinical scanner (Avanto, Siemens, Erlangen, Germany) by using a phased array coil and a vector ECG system. Cine MR images were acquired using a retrospectively ECG-gated, steady-state free precession cine MRI technique in short-axis and long-axis views of the heart using 1.2 ms echo time (TE), 40 ms repetition time (TR), 50° flip angle, 300 mm field-of-view, 8 mm slice thickness, and 256×256 image matrix. Sixteen short-axis images were acquired by using an ECG-gated, saturation recovery true fast imaging with steady state precession (FISP) sequences.

Delayed enhancement images were obtained after injection of 0.05 mmol/kg of contrast using an inversion recovery-prepared, gradient-echo sequence. Short-axis and long-axis images were obtained 10 to 15 minutes after gadolinium injection.

The images were analyzed using Mass 6.1.6 software (Medis, The Netherlands). After segmentation of the left ventricular (LV) endocardial and epicardial borders, end-diastolic, and end-systolic volumes and global LV ejection fraction were automatically calculated. The LV and infarcted myocardial mass were determined from the cine and delayed enhancement MR images, respectively. The infarct size was determined relative to LV mass.

### Histological Detection of Intramyocardially Injected MSCs

Tissue samples from the noninfarcted, infarcted-treated, and infarcted-nontreated myocardium were fixed in 4% buffered paraformaldehyde for 3 days at 4°C, and embedded in paraffin for routine histological procedures. Five-micrometer sections were counter-stained using Hoechst stain (Sigma Aldrich H6024) at 0.5 µg/mL incubated for 10 minutes.

For counting of the RFP<sup>+</sup> cells, 10 myocardial tissue blocks (injected and remote areas, 8×8×8 mm of size) were sectioned, and the sections with the appropriate depths (determined by confocal microscope) with the RFP<sup>+</sup> cells were further cut into final 15-µm slices. The total numbers of RFP<sup>+</sup> cells were counted in 200 slices of each block. The fluorescence images were acquired on a Leica TCS-SP2-AOBS confocal microscope (Leica TCS-SP2-AOBS), with a 63×/1.30 glycerol-immersion objective. An UV/HeNe laser with filter settings for DAPI/TRITC fluorescence was used for simultaneous two channels detection.

### Localization of the LV-RL-RFP-tTK-MSCs Injections

For confirmation of the location and viability of the injected cells, six pigs underwent the same protocol as the animals in Group LV-RL-RFP-tTK-MSC, but received the LV-RL-RFP-tTK-MSC intramyocardially using NOGA guidance in two sites ( $0.72\pm 0.25\times 10^6$  cells/injection site) with an additional injection of nontransfected MSCs in the opposite posterior wall. <sup>13</sup>N-ammonia PET followed by [18F]-FHBG PET-CT scans was performed 8 hours (n=3) or 7 days (n=3) after MSC delivery (Figure 2).

Additionally, transmission PET scans were registered to the corresponding MRI scans, using landmark-based registration for further confirmation of the injection sites with PET-MRI fusion software. The homologous anatomic landmarks were delineated on the contours of lung, thorax and the heart apex. The PET images were resliced by the evaluated rigid body transformations and the MRI and PET images were visualized by BrainCAD image fusion software ([www.pet.dote.hu/braincad](http://www.pet.dote.hu/braincad)).

For cell counting by luciferase assay, additional three pigs received intramyocardial injections of increasing number of LV-RL-RFP-tTK-MSC ( $0.05\times 10^6$ ,  $0.1\times 10^6$ ,  $0.2\times 10^6$ ,  $0.3\times 10^6$ ,  $0.4\times 10^6$ , and  $0.5\times 10^6$ ) into the infarct border zone, followed by euthanasia.

### Luciferase Assay

Tissue samples ( $1.52\pm 0.09$  g) collected from the infarcted (injected and noninjected) and normal myocardium and different organs of the animals were mechanically disrupted at high speed for 15 to 20 seconds in ice-cold standard relaxing solution: Na-ATP, MgCl<sub>2</sub>, ethylene glycolbis (β-aminoethyl ether)-N,N,N-tetraacetic acid (EGTA), KCl, imidazole at 4:1:2:100:10 mmol/L/L, respectively (1 g tissue/0.5 mL solution).<sup>13</sup> The homogenized tissue was centrifuged at 800 rpm for 1 minute at 4°C. The supernatant was discarded and the tissue was resuspended in standard relaxing solution containing 0.3% Triton X-100 for 6 minutes to remove membranous structures. After washing twice with the relaxing solution,



the cells and cell fragments were resuspended in standard relaxing solution. Luciferase was determined using components of the Dual-Luciferase Reporter Assay System (Promega, Madison, Wisconsin, USA). Briefly, an equal volume of passive lysis buffer was added to the homogenized tissue samples, and incubated 15 minutes at room temperature. Luciferase was measured in a Luminoscan Ascent luminometer (Labsystems) and expressed in relative light units (RLU) per  $\mu\text{g}$  protein.

### Statistical Analysis

Parameters in the LV-RL-RFP-tTK-MSCs treated animals and controls were expressed as means  $\pm$  standard deviation. The analysis of the quantitative MRI data was performed blinded to treatment arm. Changes in MRI parameters (in Groups LV-RL-RFP-tTK-MSC and Control) and the cell doubling data were tested using an analysis of variance. The probability values yielded by the multiple comparisons were corrected for multiplicity by using the method of Bonferroni-Holm. A  $P < 0.005$  was considered statistically significant.

The authors had full access to and take full responsibility for the integrity of the data. All authors have read and agree to the manuscript as written.

## Results

### In Vitro Controls of the Transfected Cells

In vitro assays of osteogenic, chondrogenic and adipogenic differentiation were not altered by transfecting the MSCs (Figure 1). Both cell viability and proliferation assays showed no significant difference between the nontransfected MSCs and LV-RL-RFP-tTK-MSC with a cell doubling time of 3.67 and 4.05 days, respectively (Figure 1). The LV-RL-RFP-tTK-MSC stably expressed both RFP and RL for five passages as examined by fluorescence-activated cell sorting and enzyme assays, respectively.

In vitro studies of [18F]-FHBG uptake demonstrated an increasing uptake of the tracer with extended incubation (Figure 3A) in a minimum detectable concentration of  $1 \times 10^5$  MSCs/mL in vitro (Figure 3B).

### In Vivo Cell Tracking of the Intramyocardially Delivered Transfected MSCs

PET imaging demonstrated focal [18F]-FHBG tracer uptake of the anterior myocardial wall accompanied by a pattern of intense tracer foci at the local injections of the LV-RL-RFP-tTK-MSC when injected in two sites with a distance of at least 2 to 3 cm 8 hours after delivery (Figure 4). Fusion imaging of PET with MRI or CT confirmed the myocardial localization of the tracer activity presumably corresponding to the RL-RFP-tTK modified MSCs (Figure 4). Seven days after LV-RL-RFP-tTK-MSC delivery, no specific [18F]-FHBG accumulation was detected in the two injection sites.

When MSCs were injected in  $11.3 \pm 1.2$  sites (Group LV-RL-RFP-tTK-MSC) [18F]-FHBG imaging showed diffuse distribution of the tracer 30 hours after injections, but not in the controls. The count ratio of [18F]-FHBG in the entire anterior wall relative to remote myocardium was  $5.3 \pm 1.8$ . Placement of ROI on the intense tracer foci of the [18F]-FHBG uptakes, the count ratio of the [18F]-FHBG of ROI relative to remote myocardium was  $11.3 \pm 3.5$ . Comparing the [18F]-FHBG tracer uptakes between the LV-RL-RFP-tTK-MSC-treated animals and controls, the count of the entire anterior wall and injection foci were  $5.8 \pm 1.6$  and  $10.9 \pm 2.7$  times greater in the treated animals relative to the controls, respectively. Seven days after cell transplantation, PET images displayed faint focal activity in the myocardium, and a similar activity pattern in the pericardium and pleura, indicating the spreading of wandering living cells to the surrounding tissues (Figure 5). The count ratio

of [18F]-FHBG of the tracer foci relative to remote myocardium was  $2.1\pm 0.3$ , and relative to the heart of control animals  $1.8\pm 0.2$  on day 7. Placement of ROIs on the pleura and pericardial locations of [18F]-FHBG uptakes, the counts were  $1.6\pm 1.1$  times higher in the treated animals compared with the control animals.

### Effect of Cell-Based Gene Therapy on Infarct Size and Myocardial Function

One pig in each group died during MI induction. MRI at 10 days revealed a trend of a decreased end-diastolic volume (EDV) ( $P=0.07$ ), an increased ejection fraction ( $P=0.06$ ), and a statistically significantly smaller infarct size ( $P<0.005$ ) in the Group LV-RL-RFP-tTK-MSC compared with control (Table 1, Figure 6).

### Number of Engrafted LV-RL-RFP-tTK-MSC

Ten days after LV-RL-RFP-tTK-MSC implantation, fluorescence confocal microscopy of the myocardium showed the presence of RFP<sup>+</sup> cells distributed through an elongated track in the area surrounding the intramyocardial injections in Group LV-RL-RFP-tTK-MSC (Figure 7) but not in samples from control pigs. The mean RFP<sup>+</sup> cells/pig in the cardiac tissue samples was  $3.46\pm 0.72\times 10^5$ , ie,  $5.8\pm 1.1\%$  of the injected cells (Figure 7).

### Luciferase Activity

Analysis of luciferase enzyme activities revealed high level of expression of the RL gene in the myocardial injection sites 10 days after delivery and some RL expression in the remote myocardial site, pericardium, pleura, liver, spleen, mediastinal lymph nodes and bone marrow (Figure 7). Fluorescence confocal microscopy confirmed the presence of RFP<sup>+</sup> cells in a mediastinal lymph node (Figure 7).

### Discussion

Our study has demonstrated the feasibility of the transgene modification of pig MSCs for triple protein expression of a PET-reporter and fluorescent luciferase genes and the serial noninvasive in vivo tracking of intramyocardially injected MSCs in a large animal model of MI with survival up to 10 days after injection. Both, in vitro and in vivo results showed that a relatively small number of cells could be detected by PET, despite the lower spatial resolution, in comparison with MRI.

Survival and proliferation of transfected stem cells with reporter genes engrafted in the myocardium has been validated in small animals.<sup>6,7</sup> In vivo tracking of the direct intramyocardial injections of adenovirus expressing wild-type HSV1-tk reporter genes in healthy, noninfarcted pigs with clinical PET scanner was reported by Miyagawa et al,<sup>12</sup> confirming the feasibility of the in vivo visualization of PET reporters in large animal model, but without using cell carrier. To understand the fate of the stem cells in cardiac regeneration therapy, PET reporter gene imaging offers one of the only clinically translatable method for in vivo tracking of the cells and their progeny in large animal model of MI.<sup>14</sup> Previously, Cao et al<sup>15</sup> showed increased thymidine kinase activity of murine embryonic stem cells transfected with PET-reporter gene injected into the rat myocardium, which corresponded with embryonic SC proliferation and teratoma formation. In contrast, our PET study with MSCs revealed a declining number of cells consistent with minimal cell proliferation and rapid cell death after intramyocardial administration. Histological analysis confirmed the presence of the surviving LV-RL-RFP-tTK-MSCs in proximity to the original intramyocardial injection site. Given the small numbers of administered cells that survived, the reduction of infarct size by MRI in the MSC-treated animals is most likely not because of direct cardiomyocytes differentiation and repair but suggestive of a paracrine effect.

In contrast to the delivery in two sites, intramyocardial injections in 10 to 12 sites demonstrated diffuse distribution of the LV-RL-RFP-tTK-MSCs by PET image 30 hours after delivery, which is probably the consequence of (1) confluent tracer activity because of lower spatial resolution of PET and (2) the incipient cell spreading in the myocardium. The latter is supported by the findings of Blömer et al,<sup>16</sup> showing that transplant cardiomyocytes transfected with lentiviral vector green fluorescence protein not only integrated into the surrounding host tissue but also showed limited migration. Seven days later, the tracer activity of the treated hearts of our animals was very low. However,  $5.8 \pm 1.1\%$  of the LV-RL-RFP-tTK-MSC could be found by microscopy, suggesting of the detection limit of  $3 \times 10^5$  PET-reporter carrier cells in vivo versus about  $1 \times 10^5$  demonstrated in vitro.

Luciferase assay confirmed the presence of LV-RL-RFP-tTK-MSC in the intramyocardial injection sites as well as an increase in the luciferase activity in the surrounding tissues and remote organs at 10 days after delivery. Indeed, RFP<sup>+</sup> cells were detected in a mediastinal lymph node, suggesting the wandering and migration of the living cells in remote organs. The clinical relevance of this finding is that reporter gene method is able to detect biodistribution of transfected cells to distant organs that may have unwanted side effects from the cells engineered for angiogenesis, longer survival, and transdifferentiation.

We used the intramyocardial delivery of the cells, as Hofmann et al<sup>17</sup> demonstrated that intracoronary delivery resulted in <3% retention of SCs in the infarcted heart within a few hours. Similar to our results, the intramyocardial delivery of embryonic cardiomyoblasts into rat hearts using in vivo dual-isotope imaging detected about 20% engrafted cells for 96 hours.<sup>15,18</sup> However, cell retention may vary based on not only the method of delivery but also the stem cell type.

The stable transfection of the cells with lentiviral or nonviral vector carrying reporter genes might influence the cell biology and physiology. Wu et al<sup>19</sup> demonstrated, that embryonic stem cells transfected with lentiviral-triple-fusion reporters (firefly luciferase, monometric RFP and tTK) down-regulated the cell cycling, cell death, and protein and nucleic acid metabolism genes with upregulation of homeostatic and antiapoptosis genes. However, despite these transcriptional changes, their study demonstrated that the expression of the lentiviral vector of trifusion reporter gene had no significant effects on embryonic stem cell viability, proliferation, and differentiation capability in vitro and in vivo.

Even if the monitoring of cell fate is of clinical importance in cell-based regeneration therapies, the usage of reporter genes in human studies has some limitations, such as extensive molecular manipulation and genetic modification of the stem cells. The remote homing of the living cells necessitates further preclinical investigations from several aspects: (1) even if the ex vivo viral gene transfer uses a replication-defective retroviral vector, a low titer of contaminating infectious lentiviral vectors could be detected by Blömer et al, which might carry a potential hazard of undesirable viral vector shuttle<sup>18</sup>; (2) cell transfection with therapeutic gene might lead to an unwanted vascularization of remote organs, hampered by the resistance of lentiviral vectors to gene silencing. Further refinement of this method will be the elimination of viral vector use for transfection, increasing the safety of cell-based gene therapy in general.

## Limitations

Although both groups included small number of animals, the results were consistent between animals and between in vivo imaging and postmortem histological analysis.

The RFP<sup>+</sup> cells were counted by confocal microscopy, a method that is limited through autofluorescence and the sectioning of the relatively large pig heart into 10 blocks.



However, the number of counted cells corresponded well with the cell number-dependent luciferase activity presented in Figure 7. An alternative and more reliable approach would be a sex-mismatch transplant and TaqMan polymerase chain reaction on Y-chromosomes, if we did not use autologous stem cells for delivery.

The presented study was a prospective study, with its limitation of a nonblinded study design. However, the analysis of the quantitative MRI data was performed blinded to the treatment arm, and thus, the functional improvement of the infarct size is not biased.

In conclusion, we have demonstrated the feasibility of PET and optical imaging of the stable expression of the trifusion gene protein in a relevant large acute ischemic animal model. Thus, this technique demonstrates promise as an approach to translational research of cell-based gene therapy in cardiovascular disease.

### CLINICAL PERSPECTIVE

The potential clinical impact of the presented study is the demonstration of the feasibility of serial noninvasive in vivo tracking of cardially delivered stem cells transfected with the reporter gene by using multimodality optical imaging with clinical PET, CT, and MRI in a relevant experimental model of myocardial ischemia (closed-chest reperfused infarction). The model and percutaneous application of cells by a clinical system support the translatability of this study. The insertion of reporter genes into stem cells allowed the monitoring of cell fate, because the reporter is expressed as long as the cells are alive and passes to the daughter cells on cell division. This study has also confirmed the efficacy of cell-based gene therapy, showing a decrease in infarct size by percutaneous intramyocardial delivery of the cells. The study has highlighted the migratory itinerary of the cardially delivered cells, as living transplanted stem cells have been detected in remote organs. The clinical relevance of this finding is that the reporter gene method is able to detect the biodistribution of transfected cells to distant organs, where they may have unwanted side-effects from the cells engineered for angiogenesis, longer survival and transdifferentiation. The further refinement of this method will be the coupling of the imaging reporters with therapeutic genes with controlled release of angiogenic factors, and elimination of viral vector use for transfection. This method has the potential of increasing the safety and efficacy of cell-based gene therapy in human regenerative medicine in ischemic or degenerative organ disorders.

## Acknowledgments

We thank Sanjiv Sam Gambhir, MD, PhD, for receiving the trifusion gene for cell transfection in Centro de Investigació'n Cardiovascular (CSIC-ICCC), Barcelona, Spain.

### Sources of Funding

The envelope plasmid pMD-G-VSVG, the packaging plasmid pCMV-DR8.2, and the expression plasmid construct containing the renilla luciferase (RL)-red fluorescent protein (RFP)-herpes simplex truncated thymidine kinase (tTK) (LV-RL-RFP-tTK) was the kind donation of Sanjiv Sam Gambhir, MD, PhD, Departments of Radiology and Bioengineering, Stanford University. The study was supported by Verein zur Förderung der Forschung Atherosclerosis, Thrombosis, and Vascular Biology, and Verein zur Förderung der Forschung im Bereich der experimentellen und klinischen Kardiologie, Vienna, Austria.

### Disclosures

Dara L. Kraitchman received grant support from Siemens AG and research material from Boston Scientific.

## References

1. Wollert KC, Meyer GP, Lotz J, Ringes-Lichtenberg S, Lippolt P, Breidenbach C, Fichtner S, Korte T, Hornig B, Messinger D, Arseniev L, Hertenstein B, Ganser A, Drexler H. Intracoronary autologous bone-marrow cell transfer after myocardial infarction: the BOOST randomised controlled clinical trial. *Lancet* 2004;364:141–148. [PubMed: 15246726]
2. Schachinger V, Erbs S, Elsasser A, Haberbosch W, Hambrecht R, Holschermann H, Yu J, Corti R, Mathey DG, Hamm CW, Suselbeck T, Assmus B, Tonn T, Dimmeler S, Zeiher AM. Intracoronary bone marrow-derived progenitor cells in acute myocardial infarction. *N Engl J Med* 2006;355:1210–1221. [PubMed: 16990384]
3. Hill JM, Dick AJ, Raman VK, Thompson RB, Yu ZX, Hinds KA, Pessanha BSS, Guttman MA, Varney TR, Martin BJ, Dunbar CE, McVeigh ER, Lederman RJ. Serial cardiac magnetic resonance imaging of injected mesenchymal stem cells. *Circulation* 2003;108:1009–1014. [PubMed: 12912822]
4. Kraitchman DL, Bulte JW. Imaging of stem cells using MRI. *Basic Res Cardiol* 2008;103:105–113. [PubMed: 18324366]
5. Walczak P, Kedziorek DA, Gilad AA, Barnett BP, Bulte JW. Applicability and limitations of MR tracking of neural stem cells with asymmetric cell division and rapid turnover: the case of the shiverer demyelinated mouse brain. *Magn Reson Med* 2007;58:261–269. [PubMed: 17654572]
6. Wu JC, Chen IY, Sundaresan G, Min JJ, De A, Qiao JH, Fishbein MC, Gambhir SS. Molecular imaging of cardiac cell transplantation in living animals using optical bioluminescence and positron emission tomography. *Circulation* 2003;108:1302–1305. [PubMed: 12963637]
7. Ray P, De A, Min JJ, Tsien RY, Gambhir SS. Imaging tri-fusion multimodality reporter gene expression in living subjects. *Cancer Res* 2004;64:1323–1330. [PubMed: 14973078]
8. Penuelas I, Boan JF, Marti-Climent JM, Barajas MA, Narvaiza I, Saty-amurthy N, Barrio JR, Richter JA. A fully automated one pot synthesis of 9-(4-[18F]fluoro-3-hydroxymethylbutyl) guanine for gene therapy studies. *Mol Imaging Biol* 2003;4/6:415–424.
9. Ben-Haim SA, Osadchy D, Schuster I, Gepstein L, Hayam G, Josephson ME. Nonfluoroscopic, in vivo navigation and mapping technology. *Nat Med* 1996;2:1393–1395. [PubMed: 8946843]
10. Gyöngyösi M, Sochor H, Khorsand A, Gepstein L, Glogar D. Online myocardial viability assessment in the catheterization laboratory via NOGA electroanatomic mapping: quantitative comparison with thallium-201 uptake. *Circulation* 2001;104:1005–1011. [PubMed: 11524393]
11. Gyöngyösi M, Khorsand A, Zamini S, Sperker W, Strehlow S, Kastrup J, Jørgensen E, Hesse B, Tägil K, Bötter HE, Ruzyllo W, Teresińska A, Dudek D, Hubalewska A, Rućka A, Nielsen SS, Graf S, Mundigler G, Novak J, Sochor H, Maurer G, Glogar D, Sylvén C. NOGA-guided analysis of regional myocardial perfusion abnormalities treated with intramyocardial injections of plasmid encoding VEGF A-165 in patients with chronic myocardial ischemia: subanalysis of the EUROINJECT-ONE Multicenter Double-Blind Randomized Study. *Circulation* 2005;112 suppl I:I-157–I-165. [PubMed: 16159809]
12. Miyagawa M, Anton M, Haubner R, Simoes MV, Städele C, Erhardt W, Reder S, Lehner T, Wagner B, Noll S, Noll B, Grote M, Gambhir SS, Gansbacher B, Schwaiger M, Bengel FM. PET of cardiac transgene expression: comparison of 2 approaches based on herpesviral thymidine kinase reporter gene. *J Nucl Med* 2004;45:1917–1923. [PubMed: 15534063]
13. Konhilas JP, Irving TC, Wolska BM, Jweied EE, Martin AF, Solaro RJ, de Tombe PP. Troponin I in the murine myocardium: influence on length-dependent activation and interfilament spacing. *J Physiol* 2003;547:951–961. [PubMed: 12562915]
14. Frangioni JV, Hajjar RJ. In vivo tracking of stem cells for clinical trials in cardiovascular disease. *Circulation* 2004;110:3378–3384. [PubMed: 15557385]
15. Cao F, Lin S, Xie X, Ray P, Patel M, Zhang X, Dylla SJ, Connolly AJ, Chen X, Weissman IL, Gambhir SS, Wu JC. In vivo visualization of embryonic stem cell survival, proliferation, and migration after cardiac delivery. *Circulation* 2006;113:1005–1014. [PubMed: 16476845]
16. Blömer U, Gruh I, Witschel H, Haverich A, Martin U. Shuttle of lentiviral vectors via transplanted cells in vivo. *Gene Therapy* 2005;12:67–74. [PubMed: 15385952]

17. Hofmann M, Wollert KC, Meyer GP, Menke A, Arseniev L, Hertenstein B, Ganser A, Knapp WH, Drexler H. Monitoring of bone marrow cell homing into the infarcted human myocardium. *Circulation* 2005;111:2198–2202. [PubMed: 15851598]
18. Zhou R, Acton PD, Ferrari VA. Imaging stem cells implanted in infarcted myocardium. *J Am Coll Cardiol* 2006;48:2094–20106. [PubMed: 17112999]
19. Wu JC, Spin JM, Cao F, Lin S, Xie X, Gheysens O, Chen iY, Sheikh AY, Robbins RC, Tsalenko A, Gambhir SS, Quertermous T. Transcriptional profiling of reporter genes used for molecular imaging of embryonic stem cell transplantation. *Physiol Genomics* 2006;25:29–38. [PubMed: 16390873]

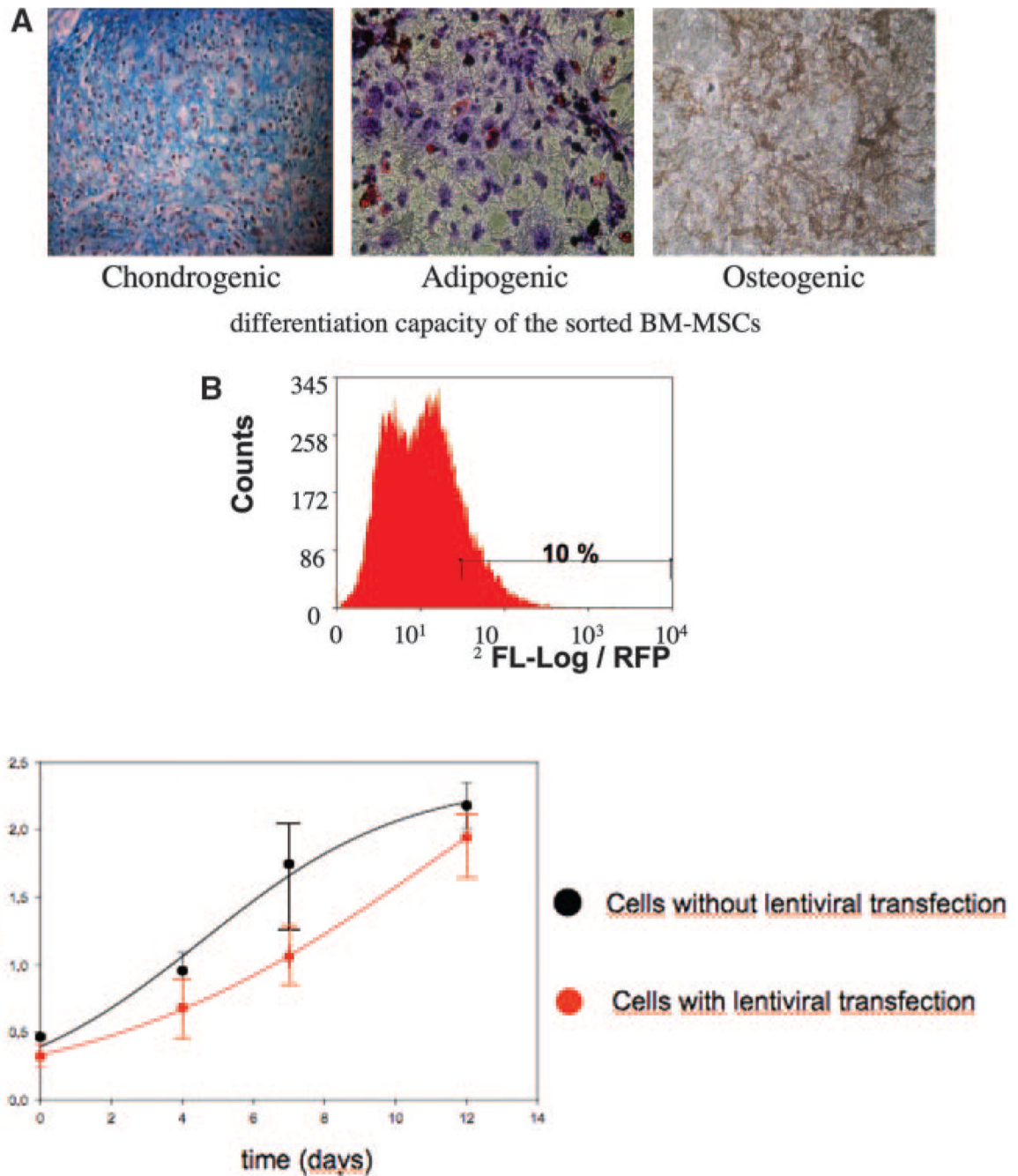


**Figure 1.**

A, Differentiation of porcine MSCs to the chondrogenic (left, alcian blue staining of proteoglycans), adipogenic (middle, oil red O staining of intracellular lipid) and osteogenic (right, von Kossa staining of mineralized calcium) cell lineages after incubation in the corresponding induction medium (magnification  $\times 20$ ). B, Fluorescence-activated cells sorting (FACS) of RFP expressing MSCs. Fluorescence intensity of the total cell population and the region corresponding to the selected 10% highest intensity fluorescing cell fraction (horizontal bar) sorted by FACS for intramyocardial delivery. C, Cell doubling time of porcine MSCs with (red) or without (black) transduction with LV-RL-RFP-tTK (mean of

4.05 days versus 3.67 days, respectively). No statistically significant difference between the groups was seen.



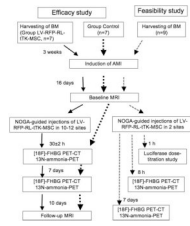


**Figure 2.** Experimental protocol and groups as a function of time. AMI indicates acute myocardial infarction.

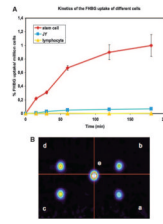


**Figure 3.**

A, In vitro [18F]-FHBG uptake kinetics based on gamma counting of pig LV-RL-RFP-tTK-MSC in comparison with nontransfected JY human B-lymphoblast and T lymphocytes. Fifteen  $\mu\text{Ci/mL}$  [18F]-FHBG was incubated with  $0.5 \times 10^6/\text{mL}$  cells for 20 to 180 minutes. Decay corrected activity is expressed as the percentage of the extracellular [18F]-FHBG incorporated per million cells. B, PET of different concentrations (a,  $1 \times 10^5$  cells/mL; b,  $2 \times 10^5$  cells/mL; c,  $3 \times 10^5$  cells/mL; d,  $5 \times 10^5$  cells/mL; e,  $1 \times 10^6$  cells/mL) of pig LV-RL-RFP-tTK-MSC labeled for 60 minutes.

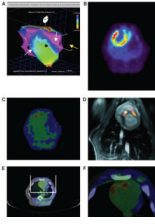


**Figure 4.**

A, Endocardial mapping of a pig heart 16 days after MI. Voltage map with the sites (black points) of the NOGA-guided intramyocardial injections of the LV-RL-RFP-tTK-MSC (white arrows at the border zone of infarction) and nontransfected MSCs (yellow arrow at the noninfarcted posterior wall). Normal viability is represented by blue and pink colors. Yellow and green color represents decreased viability in the mid-distal anterior wall and red nonviability at the heart apex. B,  $^{13}\text{N}$ -ammonia PET with transmission scan of the pig heart (supine position) 16 days after acute MI indicating perfusion defect in the anterior wall and apex. C,  $^{18}\text{F}$ -FHBG tracer uptake in the two injected points, representing the location of the LV-RL-RFP-tTK-MSC 8 hours after cell delivery into the myocardium (PET-transmission scan, pig in supine position). No activity in the posterior wall, where the nontransfected MSCs were injected. D, Fusion image of MRI (grayscale) and  $^{18}\text{F}$ -FHBG-PET (hot scale) indicating tracer accumulation in the sites only where LV-RL-RFP-tTK-MSC were intramyocardially injected. E,  $^{18}\text{F}$ -FHBG-PET-CT hybrid image for localization of the injected cells in the anterior wall. F, Magnification of the ROI of  $^{18}\text{F}$ -FHBG-CT.

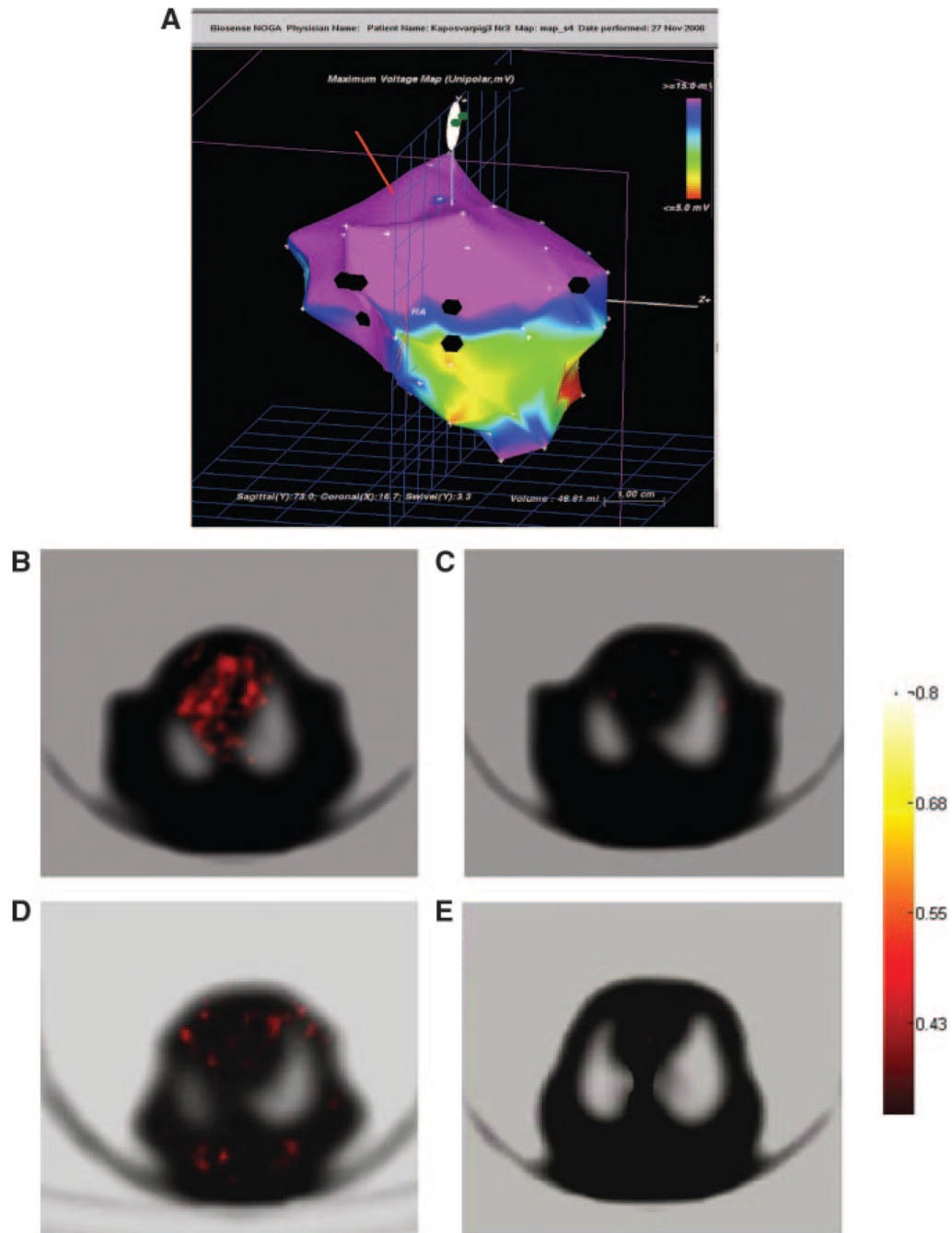


**Figure 5.**

A, NOGA endocardial mapping of pig left ventricle 16 days after MI with 12 injections (black points) of LV-RL-RFP-tTK-MSC at the border zone of anterior wall MI. B, PET image of a pig 30 hours after injection of LV-RL-RFP-tTK-MSC demonstrates diffuse high tracer activity in the myocardium, corresponding with the 12 injection sites of the transfected cells. The emission and transmission slices are represented by hot color bar and grayscale with standard uptake values. C, No uptake is detected in the control animal. D, PET images seven days after injection of LV-RL-RFP-tTK-MSCs with decreased but still detectable scattered tracer activity in the myocardium in the MSC-treated animal, and in the

surrounding tissues indicating wandering of the living cells probably through the lymphatic routes. E, No tracer accumulation in the control pig at 23 days after MI.



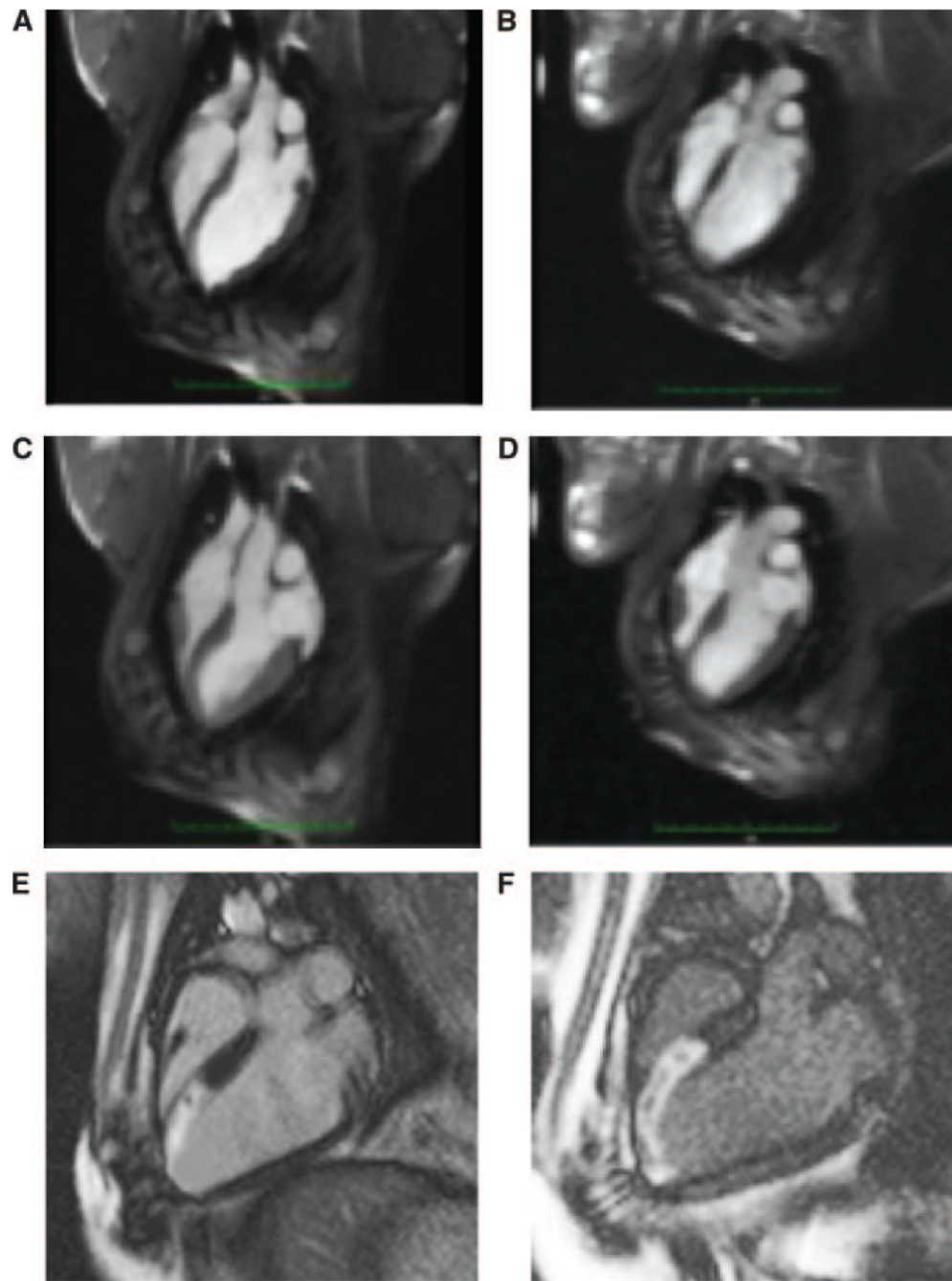


**Figure 6.** Representative MRI images of the MSC-treated (left) and control (right) animals at end-diastole (A and B, respectively) and end-systole (C and D, respectively) at 26 days after MI. A slight increase in end-diastolic volume is appreciated in the control animal relative to the MSC-treated animal. Delayed contrast-enhanced MRI demonstrates infarcted myocardium (arrows) on long-axis MRI view of the MSC-treated (E) and control (F) animals.

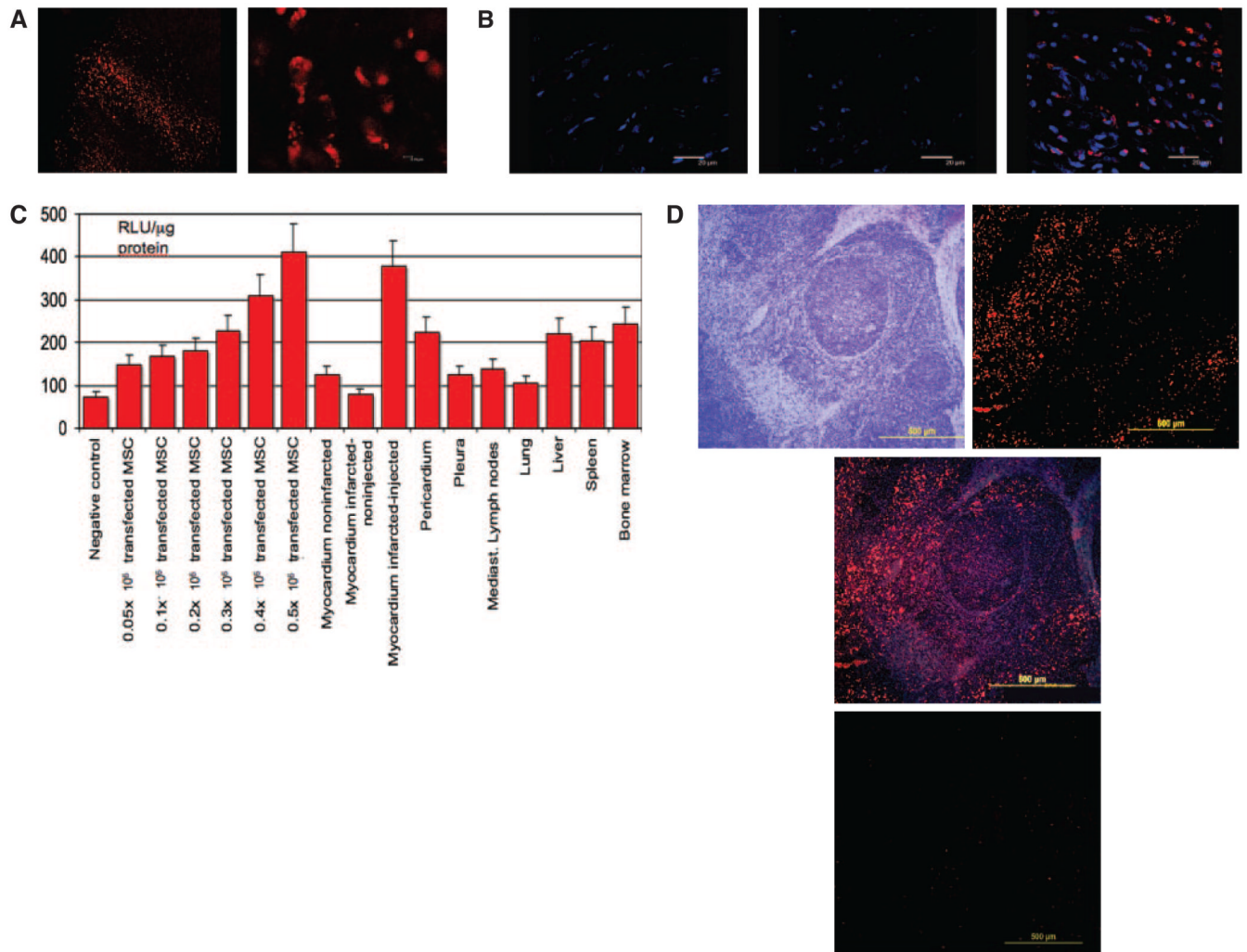


**Figure 7.**

A, Fluorescence confocal microscopy of myocardium taken 10 days after the intramyocardial LV-RL-RFP-tTK-MSC delivery. The cells are distributed through an elongated track, in the surrounding area of the intramyocardial injection (magnification  $\times 20$  and  $\times 60$ ). B, Fluorescence confocal microscopy analysis of myocardium from the central infarct zone of control animal (left), control noninfarcted myocardium (middle) and infarct zone of MSC-treated animal (right). Cell nuclei (blue) were stained with Hoechst 33258 dye. RFP expressing MSCs (red) appear only in MSC-treated animal (magnification  $\times 63$ ). C, Luciferase assay of the homogenized tissue samples 10 days ( $n=6$ ) after intramyocardial delivery of LV-RL-RFP-tTK-MSC, compared with negative control and certain number of injected transfected cells (from  $0.05 \times 10^6$  to  $0.5 \times 10^6$ ) extracted immediately after intramyocardial delivery. Parallel with the decrease of the living cells in the myocardium, small increase in luciferase activity in the other organs, indicating wandering of the living cells. RLU relative light units. D, RFP<sup>+</sup> cells in a mediastinal lymph node in a treated pig 10 days after LV-RL-RFP-tTK-MSC intramyocardial delivery. D/1: hematoxylin-eosin staining of the lymph node, D/2: RFP<sup>+</sup> cells, D/3: merge image, D/4: RFP- lymph node in a control.

Table 1

## Magnet Resonance Imaging Results

	LV-RL- RFP-tTK- MSCs- Treated	Control	<i>P</i>
Baseline			
End-diastolic volume (ml)	80.9±7.6	80.0±6.2	0.81
Ejection fraction (%)	42.6±3.9	43.7±5.9	0.69
Left ventricular mass (g)	85.2±4.4	85.0±7.9	0.96
Infarcted myocardial mass (g)	25.0±4.0	24.9±3.7	0.96
Infarct size (%)	29.4±5.0	29.5±5.2	0.98
Follow-up			
End-diastolic volume (ml)	80.0±4.4	88.0±7.7	0.07
Ejection fraction (%)	46.9±3.0	43.5±2.3	0.06
Left ventricular mass (g)	88.9±3.2	90.3±4.5	0.57
Infarcted myocardial mass (g)	20.7±1.5	27.3±3.1	<0.005 <sup>‡</sup>
Infarct size (% of LV)	23.3±1.5 <sup>*</sup>	30.2±3.5	<0.005 <sup>‡</sup>

Uncorrected *P* values are reported.

\* *P*=0.024 between baseline and follow-up within the group.

<sup>‡</sup> Represent significant differences between the groups after Bonferroni-Holm multiplicity test corrections.